Poly(ether urethane) Networks from Renewable Resources as Candidate Biomaterials: Synthesis and Characterization

Gerard Lligadas, Joan C. Ronda,* Marina Galià, and Virginia Cádiz

Departament de Química Analítica i Química Orgànica, Universitat Rovira i Virgili, Campus Sescelades, Marcellí Domingo s/n, 43007 Tarragona, Spain

Received October 9, 2006; Revised Manuscript Received November 16, 2006

A series of poly(ether urethane) networks were synthesized from epoxidized methyl-oleate-based polyether polyol and 1,3-propandiol using L-lysine diisocyanate as a nontoxic coupling agent. Polyurethanes with different hard segment contents were prepared to tune the final properties of the materials. The polyurethanes were fully chemically and physically characterized, including water uptake and in vitro hydrolytic degradation measurements. The weight loss of the polyurethanes was traced, and the changes in the surface morphology with the degradation time were examined by scanning electron microscopy. The experimental results revealed that the hard segment content is the main factor that controls the physical, mechanical, and degradation properties of these polymers. The observed diversity in material properties suggests that these polyurethanes may be useful for a wide range of biomedical polymer applications.

Introduction

Biodegradable polymers are receiving more and more attention due to their wide application in biomedical uses.[1] They may act as temporary scaffolds to facilitate tissue regeneration or replacement and may also be used for temporary therapeutic purposes, eliminating the need for subsequent removal.[2,3] The majority of the biodegradable polymers developed in the last two decades were aimed at either drug delivery systems[1] or fracture fixation devices and are typically hard, rigid materials.[4] In contrast, few biodegradable elastomers have been synthesized, and new materials are required to meet the need for an increasingly diverse range of physical properties. Biodegradable elastomers are expected to be suitable for any application requiring the use of a flexible, elastic material, such as soft tissue engineering.

Segmented polyurethane elastomers have been used as biomaterials for several decades in the fabrication of medical implants such as cardiac pace makers and vascular grafts because of their unique physical properties and relatively good biocompatibility.[5] Segmented polyurethanes are elastomeric block copolymers that generally exhibit a phase-segregated morphology made up of soft rubbery segments and hard glassy or semicrystalline segments.[6] The soft segment usually consists of polyether or polyester diols whereas the hard segment consists of the diisocyanate component and a low molecular weight chain extender. The advantage of segmented polyurethanes is that their segmental and domain structure can be controlled over a considerable range through the selection of the materials, their relative proportions, and the processing conditions.

Segmented polyurethanes can also be designed to have chemical linkages that are degradable in the biological environment, and there has been some interest in developing degradable polyurethanes for medical applications such as scaffolds for tissue engineering.[7−9] In addition to the physical properties, great care has to be taken in the choice of building blocks. Their degradation products have to be biocompatible, nontoxic, and metabolized or eliminated by the living organism. Convenient long-chain diols are polyethers such as polyethylene oxide diols or polyesters such as polycaprolactone, due to its good biocompatibility and biodegradability. However, a major problem has been the toxicity of degradation products, particularly those derived from the aromatic diisocyanate component, as carcinogenic and mutagenic aromatic diamines have been reported as potential degradation products.[5] Accordingly, in designing degradable polyurethanes, diisocyanates such as L-lysine diisocyanate (LDI) have been used.[7,10−12] Bruin et al. reported that if the hydrolysis of the urethane bonds of the polymer takes place during degradation, then the product would be a lysine derivative, an essentially nontoxic product.[10]

The design of polymers from renewable resources is currently receiving increasing attention and interest has focused on the use of cheap, biodegradable, and annually renewable starting materials to reduce petroleum dependence and the negative impact on the environment.[13] Vegetable oils and fatty acids are one of the cheapest and most abundant biological sources available in large quantities, and their use as starting materials has numerous advantages, including low toxicity and inherent biodegradability.[14] In recent years, extensive work has been done to develop polymers from triglycerides or fatty acids as the main component.[15]

Polyols derived from vegetable oils are raw materials from renewable resources and can be used in the preparation of polyurethane products. For natural oils to be used as raw materials for polyol production multiple hydroxyl functionality is required. Different ways of preparing vegetable-oil-based polyols have been successfully developed: epoxidation and further oxirane ring opening,[16] hydroformylation,[17] ozonolysis,[18] or reaction at the double bonds and subsequent reduction of the carboxyl groups.[19]

To further extend the applications of these renewable resources, our group has focused on converting vegetable oils into useful biopolymers. In a previous study, we described the synthesis of polyether polyols through the combination of cationic polymerization of epoxidized methyl oleate (EMO) and

* Author to whom correspondence should be addressed. E-mail: juancarlos.ronda@urv.cat.

10.1021/bm060977h CCC: $37.00
Published on Web 01/05/2007

Chart 1. Chemical Structures of P184, PDO, and LDI.

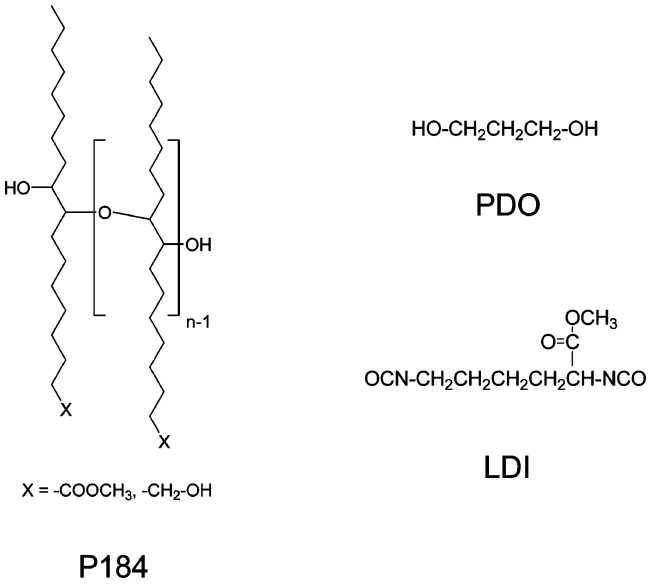

the reduction of carboxylate groups to hydroxyl moieties. Polyols with different hydroxyl contents were obtained and reacted with methylene di-*p*-phenylene isocyanate (MDI) to yield polyurethanes that behave like hard rubbers or rigid plastics.[19] We have also developed novel biobased silicon-containing polyurethanes from these polyols and silicon-containing polyols with terminal primary hydroxyl groups.[20]

On the basis of these premises, in this study we synthesized a series of polyurethane elastomer networks based on EMO, polyether-polyol (P184) with OH number = 184 mg KOH/g, L-lysine diisocyanate (LDI), and 1,3-propandiol (PDO) as a chain extender that can be obtained from rapeseed oil production in the presence of *Clostridium butyricum*[21] or from corn.[22] Their chemical structures, molecular characteristics, and thermal properties were studied using ^{13}C NMR, Fourier transform infrared (FTIR), wide-angle X-ray diffraction (WAXD), differential scanning calorimetry (DSC), dynamic mechanical thermal analysis (DMTA), and thermogravimetric analysis (TGA). In view of the future application of the synthesized polyurethanes in the biomedical field, water uptake and in vitro degradation studies were carried out, and the morphology of the degraded polyurethanes was observed by scanning electronic microscopy (SEM).

Experimental Section

Materials. Epoxidized methyl-oleate-based polyether polyol (P184) with OH number = 184 mg KOH/g was synthesized in our laboratory using the procedure described earlier.[19] This OH number corresponds to the equivalent weight of the polyol, 305 g/equiv, functionality, 3.8, and molecular weight, 1187 g/mol. The diisocyanate chosen was 2,6-diisocyanato methyl caproate (L-lysine diisocyanate, LDI) (Kyowa Hakko Kogyo Co.). Stannous 2-ethylhexanoate (95%) was purchased from Aldrich and was used as received. Chain extender 1,3-propandiol (>98%) was purchased from Aldrich and was distilled and stored at ambient temperature in a dessecator until used.

Synthesis of Polyurethanes. Polyurethanes were prepared using a single-stage process. After 5 min of mixing the appropriate amount of EMO-based polyether polyol (P184), chain extender (PDO), and diisocyanate (LDI) (Chart 1) under nitrogen at room temperature, a small amount of the catalyst (0.001 wt % of stannous 2-ethylhexanoate) was added, and then additional mixing for 30 s was conducted. Approximately 1% weight of excess LDI (NCO/OH ratio = 1.02) was used for the completion of the reaction. The mixture was poured into a preheated open mold and cured for 2 h at 60 °C and then postcured at 110 °C overnight. Circular silanized glass molds of 3 cm in diameter were used. Chemical composition and hard segment content of the polyurethanes are shown in Table 1. From the sample code in Table 1, the number denotes the hard segment percentage of the polyurethanes.

Table 1. Chemical Composition of Polyurethane Networks

sample code[a]	P184 (g)	PDO (g)	LDI (g)	% hard segment[b]
PU	5	0	1.73	
PU-31	5	0.15	2.14	31.4
PU-42	5	0.5	3.11	41.9
PU-52	5	1.0	4.48	52.3

[a] The number in the sample code denotes the hard segment % wt of the PU. [b] The hard segment percentage is calculated as the wt % of PDO and LDI per total material weight.

Characterization. The NMR spectra of the oil samples were recorded on a Varian Gemini 400 MHz spectrometer (400 MHz for ^1H and 100.57 for ^{13}C). The samples were dissolved in deuterated chloroform, and ^1H NMR and ^{13}C NMR spectra were obtained at room temperature using tetramethylsilane as the internal standard. The IR spectra were recorded on a Bomem Michelson MB 100 FTIR spectrophotometer with a resolution of 4 cm^{-1} in absorbance mode. An attenuated total reflection (ATR) accessory with thermal control and a diamond crystal (Golden Gate heated single-reflection diamond ATR, Specac-Teknokroma) was used to determine the FTIR spectra.

Calorimetric studies were carried out on a Mettler DSC822e thermal analyzer with N_2 as the purge gas. The heating rate was 20 °C/min. T_g was determined from the second heating scan of the DSC measurements as the temperature of the halfway point of the jump in the heat capacity. Thermal stability studies were carried out on a Mettler TGA/SDTA851e/LF/1100 with N_2 as the purge gas at scanning rates of 10 °C/min.

WAXD measurements were made using a Siemens D5000 diffractometer (Bragg−Brentano parafocusing geometry and vertical $\theta-\theta$ goniometer) fitted with a curved graphite diffracted-beam monochromator, incident- and diffracted-beam Soller slits, a 0.06° receiving slit, and a scintillation counter as a detector. The angular 2θ diffraction range was between 1° and 40°. Samples were dusted onto a low background Si(510) sample holder. The data were collected with an angular step of 0.05° at 3 s per step. Cu Kα radiation was obtained from a copper X-ray tube operated at 40 kV and 30 mA.

Mechanical properties were measured with a dynamic mechanical thermal analyzer (TA DMA 2928). Specimens 1.2 mm thick, 5 mm wide, and 5 mm long were tested in a three-point bending configuration. The various thermal transitions were studied between −100 and 100 °C at a heating rate of 2.5 °C/min and a fixed frequency of 1 Hz.

SEM was performed on a JEOL JSM 6400 scanning electron microscope at an activation voltage of 15 kV. The polymeric samples were mounted on a sample holder and were sputter-coated under vacuum with graphite.

Hydrophilicity of Polyurethanes. The hydrophilicity of the polyurethanes was quantified by the measurement of the amount of water that each polymer absorbed at 37 °C. The samples (1 × 1 × 0.1 cm) were immersed in distilled water and were kept at 37 °C. The samples were removed from water at predetermined time intervals, wiped gently with filter paper, and weighed with an analytical balance. After the samples were dried under vacuum at 60 °C, the weight of the dry samples was determined. The water uptake was defined as follows: water uptake (wt %) = $100(W_w - W_d)/W_d$, where W_w represents the weight of the wet sample after immersing and W_d represents the weight of the sample after drying.

In Vitro Degradation of Polyurethanes. Each sample (1 × 1 × 0.1 cm^3) was placed in an individual test bottle and kept at 37 °C in phosphate-buffered saline (PBS, 0.1 M, pH 7.4). PBS was changed at each analysis point. The degradation rate was determined by the weight loss over predetermined time intervals. Weight loss was defined as

follows: weight loss (%) = $(W_0 - W_t)/W_0 \times 100$, where W_0 represents the weight of the dry sample before degradation and W_t represents the weight of the dry sample after degradation at different time intervals.

Results and Discussion

Synthesis of Polyurethanes. One of the most widely used techniques to obtain polyurethanes is the one-shot technique, which consists of the very efficient mixing, in one step only, in a short time, of all of the raw materials involved in polyurethane preparation: polyol, chain extender, and isocyanate.[6]

In this study, novel segmented biobased polyurethanes were prepared using the one-shot technique from epoxidized methyl-oleate-based polyether polyol (P184) with OH number = 184 mg KOH/g, LDI, and PDO as a chain extender. As has been previously described, P184 was obtained from methyl oleate by the epoxidation of carbon double bonds, cationic oligomerization of the resulting epoxy fatty acid ester, and partial reduction of the ester groups.[19] The chemical structure and the characteristics of the materials are shown in Chart 1. When synthesizing polyurethanes, aliphatic diiisocyanates have a lower reactivity than aromatic ones, and a catalyst is necessary to speed up the reaction with polyols. However, catalysts such as amines or organometallic compounds may be highly toxic. Among them, stannous 2-ethylhexanoate (commonly referred as stannous octoate) is a good choice on the basis of its acceptance by the Food and Drug Administration as a catalyst in the formulation of polymeric coatings in contact with food.[23]

The chemical composition and hard segment content of the synthesized polyurethanes are shown in Table 1. The molar composition of P184 was set at 1.0, and then the molar ratio of PDO and LDI was varied to obtain polyurethanes with different hard segment contents. The NCO/OH molar ratio was kept constant at 1.02 to compensate for isocyanates that are consumed in side reactions during the urethane synthesis, and reactants were mixed at 60 °C and cured at this temperature for 2 h before being postcured at 110 °C overnight to give the polyurethanes. ^{13}C NMR and FTIR spectroscopies were used to monitor the isocyanate to urethane conversion. The ^{13}C NMR spectra for P184, LDI, and the swollen PU-52 with all of the assignments are shown in Figure 1. The isocyanate peaks essentially disappear upon conversion to the urethane, and new resonances assigned to the carbonyls of the newly formed carbamates appear at 156 ppm. FTIR analysis also demonstrated the urethane formation reaction during polymer synthesis. The disappearance of the absorption band at 2240 cm^{-1} assigned to the isocyanate group indicated that the reaction was complete, and their urethane structure was demonstrated by absorption bands at around 3412 cm^{-1} (N−H stretching), 1530 cm^{-1} (C−N stretching, combined with N−H out-of-plane bending), and 1725 cm^{-1} (C═O stretching). A small absorption band at around 1663 cm^{-1} was due to the formation of urea linkages, which may be the reaction of some of the unreacted isocyanates with the atmospheric moisture while curing as a side reaction.

Structural Analysis of Polyurethanes. To investigate the molecular structure of polyurethanes, WAXD and FTIR spectroscopy were employed. All samples show similar WAXD curves with a large wide diffraction halo at around 20°, which is typical for amorphous polymeric materials. It seems that the nonsymmetrical diisocyanate LDI that also contains a methyl ester side chain produces hard segments that were unable to pack efficiently to form a crystalline hard segment domain. FTIR spectroscopy was used to investigate the structural difference in hard and soft segments of synthesized polyurethanes with

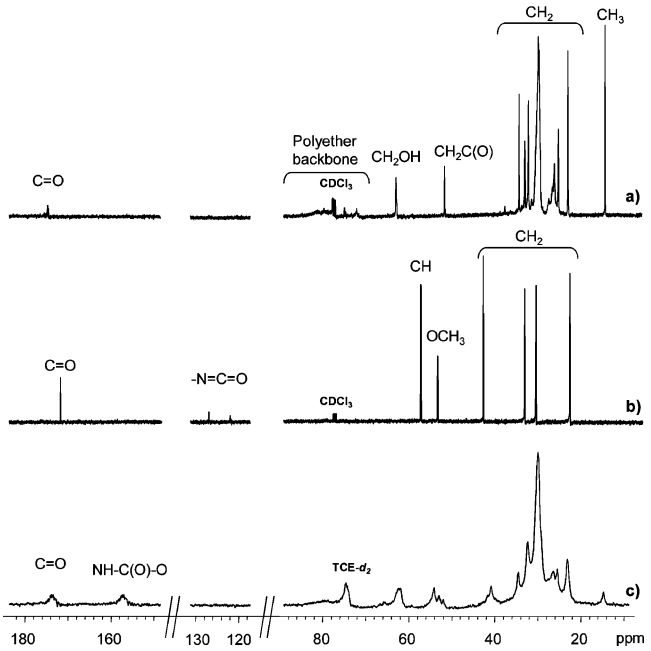

Figure 1. ^{13}C NMR (100 MHz) spectra of (a) P184 ($CDCl_3$), (b) LDI ($CDCl_3$), and (c) swollen PU-52 (TCE-d_2).

various PDO fractions. Almost all of the infrared research on polyurethanes has focused on two principal vibrational regions: the N−H stretching vibration (3200−3500 cm^{-1}) and the carbonyl C═O stretching vibration amide I region (1700−1730 cm^{-1}).[24,25] Polyurethanes are capable of forming several kinds of hydrogen bonds due to the presence of a donor N−H group and a C═O acceptor group in the urethane linkage. The oxygen atom of the ester or ether linkage when a polyester or a polyether soft segment is present may also act as a proton acceptor. Therefore, hard segment−hard segment or hard segment−soft segment hydrogen bonding can exist. These bands have been widely used to characterize, at least semiquantitatively, the hydrogen bonding state of the polymer and to correlate this to the phase separation in the system. It is well-known that in hydrogen-bonded urethane N−H and C═O bands appear at lower wavenumbers than those in free ones.[26] Figure 2 shows the FTIR spectra of C═O and N−H stretching vibration regions for the synthesized polyurethanes. The band at 1735 cm^{-1} is ascribed to the C═O stretching of LDI and the remaining methyl ester groups of the polyether polyol, the broad band between 1730 and 1672 cm^{-1} is attributable to associated and nonassociated C═O urethane groups, and the small shoulders at 1663 and 1643 cm^{-1} are ascribed to associated and nonassociated urea linkages. Analysis of the amide I stretching vibration for a PU sample indicates that there is a band at approximately 1720 cm^{-1}, which is attributable to free C═O urethane groups, and a shoulder at about 1695 cm^{-1}, which is due to the hydrogen-bonded urethane. The intensity of the bands attributed to free and hydrogen-bonded urethane carbonyls increases with increasing PDO fraction, as could be expected, because the increasing PDO fraction leads to an increased urethane content. The intensity of the band attributed to hydrogen-bonded urethane, relative to the band attributed to the nonbonded urethane groups, increases with an increase in the hard segment content. This suggests that the PU-42 and PU-52 C═O urethane groups are hydrogen-bonded to a greater degree than the PU and PU-31 samples. In the amine region (Figure 2, bottom panel), the broad band ascribed to N−H stretching grows with the increase in urethane group concentration and shifts slightly to a lower wavenumber with increasing

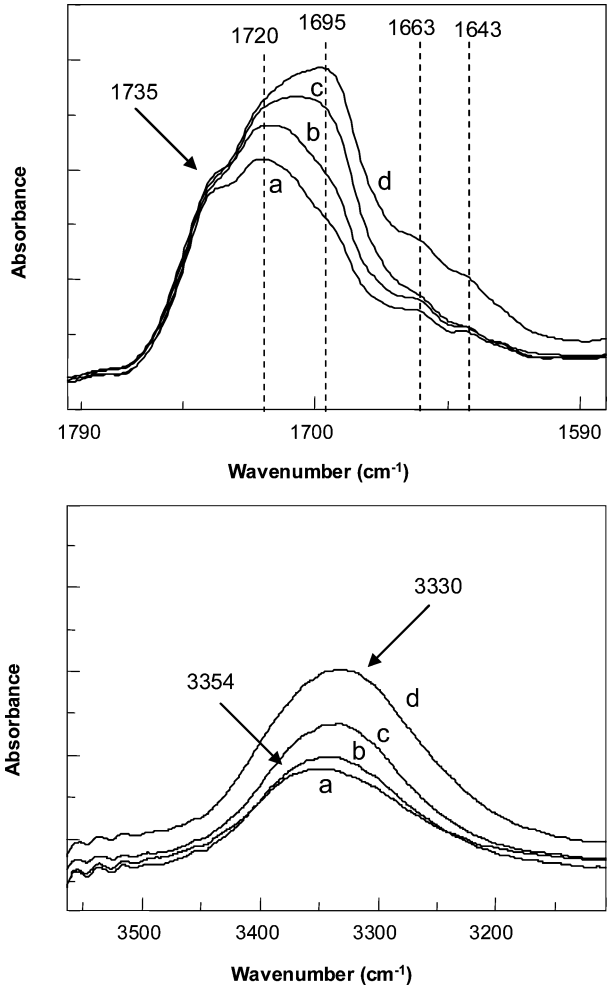

Figure 2. FTIR spectra of carbonyl (top) and amine (bottom) regions of polyurethane networks: (a) PU, (b) PU-31, (c) PU-42, and (d) PU-52.

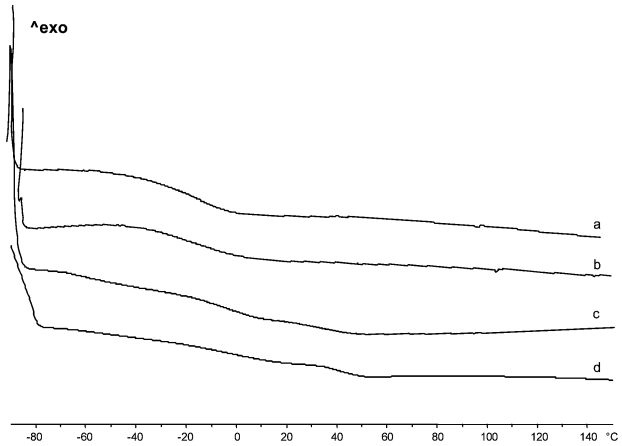

Figure 3. DSC thermograms (20 °C/min) of polyurethane networks: (a) PU, (b) PU-31, (c) PU-42, and (d) PU-52.

hard segment content, indicating an increase in the degree of association. The difference in the state of molecular aggregation of polyurethanes was further confirmed by DSC and DMTA.

Thermal Properties of Polyurethanes. Thermal analysis of the polyurethanes obtained was performed to provide insights into the morphological structure of the material. Figure 3 shows the second heating DSC thermogram for the polyurethanes, while thermal transitions are listed in Table 2. No melting or crystallization peaks were found by DSC, which is in full agreement with the WAXD observation. The glass transition temperature of the reference sample measured by DSC was −17 °C. DSC thermograms of all polyurethanes extended with PDO showed a low-temperature glass transition, indicated by an endothermic step in the heat flow. Such transitions appeared in the region from −15 to 5 °C and were attributed to the P184 soft segment glass transition temperature (T_{g1}). The T_{g1} value is a measure of the relative purity of the soft segment regions; when there are hard segments dispersed in the soft domains, the T_{g1} value is increased. The degree of hard segment mixing into the soft segment domain will depend on the overall hard segment content and the affinity of one segment toward the other. In our polyurethanes, hard segment content is high enough to achieve phase separation, but the hard segment has a highly irregular aliphatic structure, meaning that phase mixing is more likely than phase separation. As indicated in Figure 3 and Table 2, the T_{g1} value increased with the hard segment content. Thus, the experimental results revealed that the dispersion of hard segments in the soft domain increased with the hard segment content. Apart from this, samples with higher hard segment content (PU-42 and PU-52) revealed a second transition (T_{g2}). This second T_g with midpoints at approximately 35 and 44 °C, respectively, was assigned to the PDO−LDI hard block of the polyurethane and supports the development of a phase-separated morphology. Glass transition temperatures for the hard segment depend strongly on its molecular weight; it can therefore be stated that the lower T_{g2} value in the PU-42 sample could be a consequence of shorter PDO−LDI segments such as could be expected from hard segment content. The enhanced phase separation noted for PU-42 and PU-52 by DSC would indicate that the higher degree of hydrogen bonding observed by FTIR (Figure 2) must be attributed to interchain interactions in the hard segments. The phase mixing noted for PU-31 by DSC would indicate that the hydrogen bonding observed by FTIR for the urethane C═O groups is largely hard segment−soft segment or soft segment−soft segment.

The dynamomechanical behavior of the polyurethanes was investigated by DMTA to obtain further evidence on morphology since this technique is more sensitive for detecting glass transitions than DSC. Figure 4a shows the elastic modulus (E') as a function of the temperature. As can be seen polyurethanes PU and PU-31 behave like homogeneous polymeric networks with respect to E'curves while PU-42 and PU-52 samples show E' curves typical of a phase-separated structure. In the glassy region, the storage moduli follow the expected trends. The storage moduli E' is higher when the hard segment content is higher due to the increased number of urethane connections and the increase in interchain interactions caused by the hydrogen bonds. At approximately 30 °C the storage moduli for the PU-42 and PU-52 samples are higher than those for the PU and PU-31 samples. It appears that the hard segments play the role of physical cross-links and fillers. Figure 4b shows the dissipation factor tan δ curves as a function of temperature. The reference sample shows a tan δ peak at 9 °C assigned to the glass transition of the amorphous soft segment. The glass transition temperature determined from the peak of the tan δ curve is higher than the one determined by DSC (Table 2), which can be related to the heat-transporting hysteresis for large scale samples in DMTA. Consistent with DSC results, this peak shows a shift of the maxima and decreasing height as the hard segment content increases (curves b, c, and d). This suggests greater limitations on freedom of chain mobility in the soft segment, which may be explained by the phase mixing between hard and soft segments. The tan δ curves of the PU-42 and

Table 2. Thermal Characterization of Polyurethane Networks from DSC, DMTA, and TGA

		DSC (°C)		DMTA (°C)		TGA (°C)	
sample code[a]	% hard segment[b]	soft segment transition (T_{g1})	hard segment transition (T_{g2})	soft segment transition (T_{g1})	hard segment transition (T_{g2})	$T_{5\%\ loss}$[c]	T_{max}[d]
PU		−17		9		297	429
PU-31	31.4	−12		14		282	284/438
PU-42	41.9	0	35	22	45	273	273/432
PU-52	52.3	1	44	21	58	255	260/434

[a] The number in the sample code denotes the hard segment % wt of the PU. [b] The hard segment percentage is calculated as the wt % of PDO and LDI per total material weight. [c] Temperature of 5% weight loss. [d] Temperature of the maximum weight loss rate.

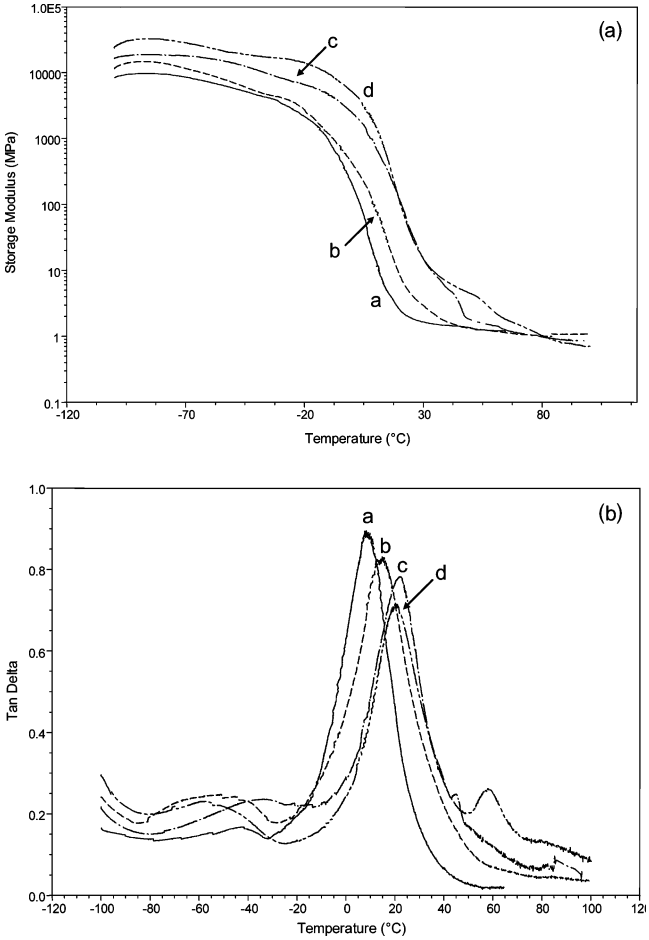

Figure 4. Storage modulus (E') and loss factor (tan δ) of polyurethanes: (a) PU, (b) PU-31, (c) PU-42, and (d) PU-52.

PU-52 samples display smaller but distinct transitions at 45 and 58 °C, respectively. This transition is attributed to T_g of the phase-separated LDI−PDO hard block segments of the polymer (T_{g2}). This transition becomes much more prominent in PU-52 due to its more phase-separated morphology. Moreover, all tan δ curves show a low-temperature transition (below −20 °C). The origin of this peak is not known, but it is generally attributed to rotation of smaller groups in the main chain.[18] This peak is larger and is at a lower temperature in the segmented polyurethanes than in the reference sample. This relaxation at a similar temperature was observed in other polyurethanes from vegetable-oil-based polyols.[19] DMTA results corroborated the DSC results, indicating that the P184 soft segment phase exists in a relatively more phase-mixed state as the hard segment content increases. These results indicate that these materials would be useful in low-temperature applications from approximately −20 °C up to around body temperature.

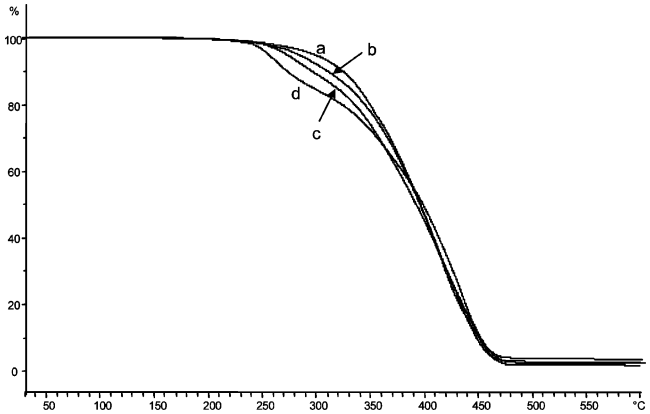

Figure 5. TGA plots (10 °C/min) of polyurethane networks: (a) PU, (b) PU-31, (c) PU-42, and (d) PU-52.

The TGA was performed on the polyurethanes under nitrogen atmosphere. The reported TGA of petroleum and vegetable-oil-based polyols suggest that thermal stability is poor.[20] The TGA thermograms of polyurethanes are shown in Figure 5, and TGA data are listed in Table 2. The thermal decomposition of these polyurethanes involves at least two overlapping steps: a small drop below 300 °C followed by the main loss weight above 300 °C. The first weight loss is related to the decomposition of the urethane bonds, which takes place through the dissociation to isocyanate and alcohol, the formation of primary amines and olefins, or the formation of secondary amines.[27] The main decomposition process is attributed to the polyether polyol chain scission and occurs at approximately 430 °C. The weight loss in the first step increases as the hard segment content increases, which is in accordance to the existence of a higher amount of weaker urethane bonds.

Water Absorption and In Vitro Degradation. Water absorption was measured to determine the polyurethane bulk hydrophilicity because this parameter was expected to have a substantial impact on hydrolytic degradation. The water uptake as a function of time for all of the samples is shown in Figure 6. Water uptake of the polyurethane obtained from P184 and MDI (PUMDI)[19] was also measured for comparison. The water uptake increased with immersion time and reached a plateau after approximately 25 h. The hard segment content is the main factor that controls the amount of absorbed water. As the hard segment content increases, a more hydrophilic character in the final network due to the presence of a higher amount of urethane groups can be expected, thus increasing the water uptake. According to this, similar water uptakes can be observed for PU and PUMDI, which contain similar amounts of urethane links.

The in vitro degradation experiments of the synthesized polyurethanes were carried out by immersion of the samples in PBS (pH 7.4, 0.1 M) at 37 °C, and the results are plotted in

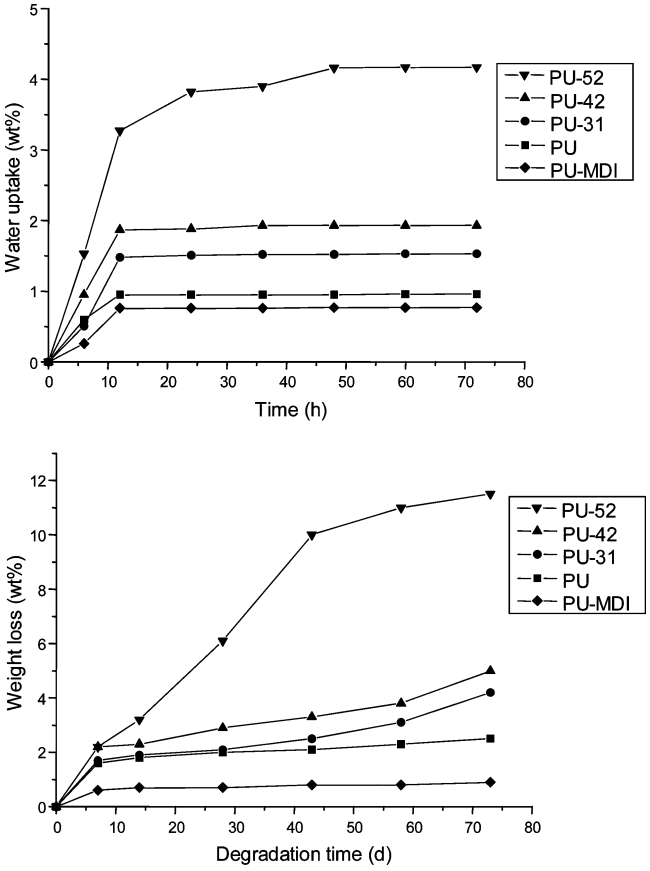

Figure 6. Water uptake (top) and in vitro degradation (PBS, 0.1 M, pH 7.4, 37 °C) (bottom) of polyurethane networks.

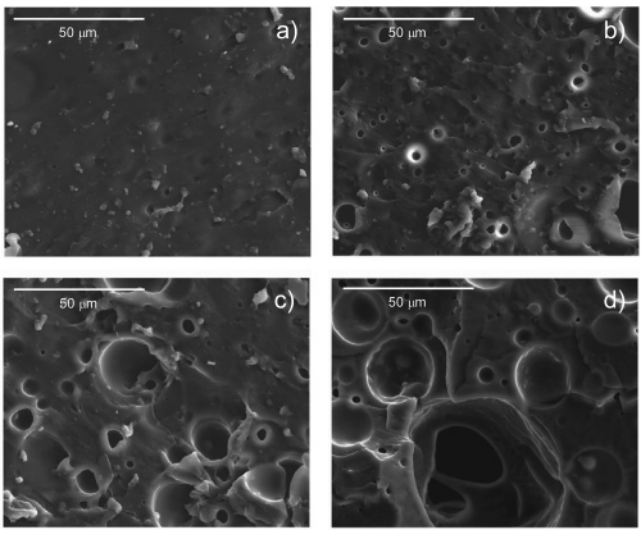

Figure 7. SEM images of degraded polyurethane PU-52 at different degradation stages: (a) 14, (b) 28, (c) 43, and (d) 73 days.

Figure 6. The degradation rate was evaluated by the weight loss of the polymers over predetermined time intervals. After 72 days of degradation, the weight losses of polyurethanes are all below 12%. As shown in Figure 6, the hard segment content has some influence on the hydrolytic degradation rate. With the increase of the hard segment content, the degradation rate increased, which is in agreement with the hydrophilicity of the polymers. The reason may be that the resulting polyurethanes containing higher hard segment content have more hydrophilicity and water diffusion is relatively easy. However, the PUMDI sample shows a lower degradation rate than that of PU in spite of their similar hydrophilicity, which can be expected from the aromatic character of MDI.

The visual examination of the surface of the degraded polyurethanes was carried out using SEM. Figure 7 shows photographs of PU-52 at different degradation stages. For all samples, the surface appeared spotted with round pits where material had been removed and showed more extensive cracks and numerous pores in progressive weeks, indicating a larger extent of degradation with time. Moreover, with the increase of the hard segment content, the erosion was more serious. The spotted surface is due to the presence of areas with marked differences in hydrolytic stability. The hydrophobic character of the soft segments prevented the entry of water molecules, resulting in greater hydrolytic stability of the polyurethane. Hard segments increase the hydrophilicity and promote the susceptibility of urethane bonds to hydrolysis, leading to the formation of significant amounts of water-soluble products leaching into the solution and to a higher degradation rate.

Conclusions

A variety of novel poly(ether urethane) networks were synthesized from EMO-based polyether polyol, PDO, and LDI as a nontoxic coupling agent with a hard segment content between 31.4% and 52.3%. The synthesized materials were exhaustively characterized by spectroscopic techniques, WAXD, DSC, and DMTA. WAXD and DSC results showed that the use of nonsymmetric and methyl ester side chain containing LDI inhibits any hard segment crystallinity. However, the significant hydrogen bonding of the urethane groups noted by FTIR as well as T_g values obtained by DSC and DMTA indicate that the polyurethanes were phase-segregated to varying degrees. Degradation behaviors were found to depend strongly on the hard segment content, as the hydrophilicity promotes the susceptibility to hydrolysis and leads to a higher degradation rate. The wide range of material properties that were achieved as well as the use of a potentially nontoxic diisocyanate make these degradable polymers useful for a variety of biomaterials applications. Moreover, these biobased polyurethanes were prepared using 100 wt % of biorenewable materials, which shows that is possible to exploit renewable resources to manufacture original and useful materials.

Acknowledgment. The authors gratefully acknowledge the Comisión Interministerial de Ciencia y Tecnología (Grant No. MAT2005-01593) for financial support for this work. G.L. acknowledges the Departament d'Universitats, Recerca i Societat de la Informació and Fons Social Europeu for a predoctoral grant (2003FI00765). We thank F. Guirado for WAXD measurements and M. Moncusí for SEM analysis. The donation of LDI by A. Marcos is gratefully acknowledged.

References and Notes

(1) Uhrich, K. E.; Cannizzaro, S. M.; Langer, R. S.; Shakesheff, K. M. *Chem. Rev.* **1999**, *99*, 3181.
(2) Wald, H. L.; Sarakinos, G.; Lyman, M. D.; Mikos, A. G.; Vacanti, J. P.; Langer, R. *Biomaterials* **1993**, *14*, 270.
(3) Sittinger, M.; Bujia, J.; Rotter, N.; Reitzel, D.; Minuth, W. W.; Burmester, G. R. *Biomaterials* **1996**, *17*, 237.
(4) Engelberg, I.; Kohn, J. *Biomaterials* **1991**, *12*, 292.
(5) (a) Lamba, N. M. K.; Woodhouse, K. A.; Cooper, S. L. *Polyurethanes in Biomedical Applications*; CRC Press: Boca Raton, FL, 1998. (b) Gunatillake, P. A.; Adhikari, R. *Eur. Cells Mater.* **2003**, *5*, 1. (c) Wang, J.; Wagner, W. R. *Biomacromolecules* **2005**, *6*, 2833. (d) Santerre, J. P.; Woodhouse, K.; Laroche, G.; Labow, R. S. *Biomaterials* **2005**, *26*, 7457.

(6) Wirpsza, Z. *Polyurethanes: Chemistry, Technology, and Applications*; Kemp, T. J., Ed.; Ellis Horwood: New York, 1993.
(7) Storey, R. F.; Wiggins, J. S.; Puckett, A. D. *J. Polym. Sci., Part A: Polym. Chem.* **1994**, *32*, 2345.
(8) Kylma, J.; Sépala, J. V. *Macromolecules* **1997**, *30*, 2876.
(9) Zdrahala, R. J.; Zdrahala, I. J. *J. Biomater. Appl.* **1999**, *14*, 67.
(10) Bruin, P.; Venstra, G. J.; Nijenhuis, A. J.; Pennings, A. J. *Makromol. Chem. Rapid Commun.* **1988**, *9*, 589.
(11) Marcos-Fernández, A.; Abraham, G. A.; Valentín, J. L.; San Román, J. *Polymer* **2006**, *47*, 785.
(12) Hassan, M. K.; Mauritz, K. A.; Storey, R. S.; Wiggins, J. S. *J. Polym. Sci., Part A: Polym. Chem.* **2006**, *44*, 2990.
(13) (a) Yu, L.; Dean, K.; Li, L. *Prog. Polym. Sci.* **2006**, *31*, 576. (b) Kaplan, D. L. *Biopolymers from Renewable Resources*; Springer: Berlin, 1998; p 267.
(14) (a) Baumann, H.; Bühler, M.; Fochem, H.; Hisrsinger, F.; Zoeblein, H.; Falbe, J. *Angew. Chem., Int. Ed.* **1988**, *27*, 4. (b) Biermann, U.; Friedt, W.; Lang, S.; Lühs, W.; Machmüller, G.; Metzger, J. O.; Klaas, M. R.; Schäfer, H. J.; Schneiderüsch, M. P. *Angew. Chem., Int. Ed.* **2000**, *39*, 2206. (c) Eissen, M.; Metzger, J.O.; Schmidt, E. Schneidewind, U. *Angew. Chem., Int. Ed.* **2002**, *41*, 414.
(15) (a) Güner, F. S.; Yagci, Y.; Erciyes, A. T. *Prog. Polym. Sci.* **2006**, *31*, 633. (b) Lligadas, G.; Ronda, J. C.; Galià, M.; Cádiz, V. *J. Polym. Sci., Part A: Polym. Chem.* **2006**, *44*, 5630. (c) Lligadas, G.; Callau, L.; Ronda, J. C.; Galià, M.; Cádiz, V. *J. Polym. Sci., Part A: Polym. Chem.* **2005**, *43*, 6295. (d) Pelletier, H.; Belgacem, N.; Gandini, A. *J. Appl. Polym. Sci.* **2006**, *99*, 3218. (e) Uyama, H.; Kuwabara, M.; Tsujimoto, T.; Kobayashi, S. *Biomacromolecules* **2003**, *4*, 211. (f) Esen, H.; Kusefoglu, S. H. *J. Appl. Polym. Sci.* **2003**, *89*, 3882. (g) Bunker, S. P.; Wool, R. P. *J. Polym. Sci., Part A: Polym. Chem.* **2002**, *40*, 451. (h) Petrovic, Z.; Guo, A.; Zhang, W. *J. Polym. Sci., Part A: Polym. Chem.* **2000**, *38*, 4062. (i) Petrovic, Z.; Guo, A.; Javni, I. U. S. Patent 6,107,433, 2000.
(16) (a) Guo, A.; Cho, Y.-J.; Petrovic, Z. S. *J. Polym. Sci., Part A: Polym. Chem.* **2000**, *38*, 3900. (b) Zlatanic, A.; Petrovic, Z. S.; Dusek, K. *Biomacromolecules* **2002**, *3*, 1048. (c) Zlatanic, A.; Lava, C.; Zhang, W.; Petrovic, Z. S. *J. Polym. Sci., Part B: Polym. Phys.* **2004**, *42*, 809.
(17) Guo, A.; Demydov, D.; Zhang, W.; Petrovic, Z. S. *J. Polym. Environ.* **2002**, *10*, 49.
(18) Petrovic, Z.; Zhang, W.; Javni, I. *Biomacromolecules* **2005**, *6*, 713.
(19) Lligadas, G.; Ronda, J. C.; Galià, M.; Biermann, U.; Metzger, J. O. *J. Polym. Sci., Part A: Polym. Chem.* **2006**, *44*, 634.
(20) Lligadas, G.; Ronda, J. C.; Galià, M.; Cádiz, V. *Biomacromolecules* **2006**, *7*, 2420.
(21) Biebl, H.; Menzel, K.; Zeng, A. P. Deckwer, W. D. *Appl. Microbiol. Biotechnol.* **1999**, *52*, 289.
(22) Kurian, J. *J. Polym. Environ.* **2005**, *13*, 159.
(23) Food and Drugs Administration. Resinous and Polymeric Coatings. *Code of Federal Regulations*, Chapter I, Part 175, Subpart C, Section 175,300, Title 21
(24) Skrovanek, D. J.; Howe, S. E.; Painter, P. C.; Coleman, M. M. *Macromolecules* **1985**, *18*, 1676.
(25) Papadimtrakopoulos, F.; Sawa, E.; MacKnight, W. J. *Macromolecules* **1992**, *25*, 4682.
(26) Seymour, R. W.; Estes, G. M.; Cooper, S. L. *Macromolecules* **1970**, *3*, 579.
(27) Levchik, S. V.; Weil, E. D. *Polym. Int.* **2004**, *53*, 1585.

BM060977H